Synthesis and evaluation of 1,2,4-triazolo[1,5-c]pyrimidine derivatives as A$_{2A}$ receptor-selective antagonists

Bidhan A. Shinkre [a], T. Santhosh Kumar [b], Zhan-Guo Gao [b], Francesca Deflorian [b], Kenneth A. Jacobson [b,*], William C. Trenkle [a,*]

[a] Chemical Biology Unit, Laboratory of Cell Biology and Biochemistry, National Institute of Diabetes and Digestive and Kidney Diseases, National Institutes of Health, Bldg. 8, Rm. 121, NIH, NIDDK, LCBB, Bethesda, MD 20892-0810, United States
[b] Molecular Recognition Section, Laboratory of Bioorganic Chemistry, National Institute of Diabetes and Digestive and Kidney Diseases, National Institutes of Health, Bethesda, MD 20892, United States

ABSTRACT

Movement disorders such as Parkinson's disease and Huntington's disease are serious life-limiting and debilitating movement disorders. Their onset typically occurs from mid-life to late in life, and effective diagnostic techniques for detecting and following the disease course are lacking. Our goal is to develop receptor imaging agents for positron emission tomography (PET) that selectively target the most relevant subtype of adenosine receptors (AR) that are highly expressed in the striatum, that is, the A$_{2A}$ AR. To further this goal, we have synthesized and characterized pharmacologically a family of high affinity A$_{2A}$ AR ligands, based on the known antagonist, SCH 442416 (R = –Me), which have structural variability on the terminus (R = –Et, –i-Pr, –allyl, and others). A O-fluoroethyl analogue suitable for use as a PET tracer had a K_i value of 12.4 nM and was highly selective for the A$_{2A}$ AR in comparison to the A$_1$ and A$_3$ ARs.

Published by Elsevier Ltd.

Movement disorders such as Parkinson's disease (PD) and Huntington's disease (HD) are serious life-limiting and debilitating movement disorders affecting roughly 1% of the US population over age 50.[1,2] The onset of these neurodegenerative diseases typically occurs from mid-life to late in life. By the time a diagnosis is made, damage to the neuronal pathways in the brain governing movement is well-advanced. One problem is a lack of adequate diagnostic techniques for detecting and following the course of these diseases. This clearly holds true for Parkinson's disease for which there currently is no predictive genetic test. Even with respect to Huntington's disease, which is entirely of a genetic origin, there remains a need for new tools to follow the progress of the neurodegeneration and to assess the effectiveness of experimental drugs by objective criteria.

Our goal is to develop receptor imaging agents for positron emission tomography (PET) that selectively target the most relevant subtype of adenosine receptors that are highly expressed in the striatum,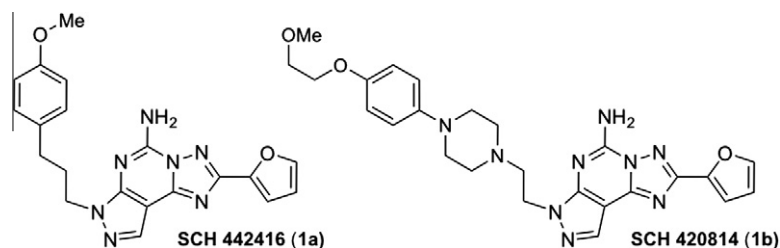 that is, the A$_{2A}$ adenosine receptor (AR).[3] Several reported selective A$_{2A}$ AR antagonists could act as starting points for development of a PET ligand including the pyrazolotriazolopyrimidine SCH 442416 (**1a**, Chart 1) and its analogue SCH 420814 (**1b**, Chart 1), which is currently in advanced clinical trials.[4–9] The A$_{2A}$ AR in the brain is distributed mainly in the striatum and the olfactory tubercle. In the striatum, adenosine acting at the postsynaptic A$_{2A}$ AR has antagonistic molecular and behavioral interactions with dopamine acting at the postsynaptic D$_2$ receptor. Thus, an antagonist of this subtype administered to a PD patient acts in a manner similar to dopamine agonists. To further the goal of developing a PET tracer, we have synthesized a family of A$_{2A}$ AR ligands based on the known antagonist, SCH 442416 (general structure **3**, R = –Me, Scheme 1), which has structural variability on the terminus (R = –Et, –i-Pr, –allyl, and others). The preparation and binding selectivity of these unreported ligands is reported herein.

The SCH 442416 pharmacophore has been previously utilized for radiolabeling experiments.[7] Specifically, the ^{11}C-labeled SCH 442416 has been successfully utilized as a PET imaging agent for the visualization of A$_{2A}$ AR in macaques (*M. nemestrina*)[7] and PD patients.[8] However, this agent suffers due to the short half-life (20.4 min) of the ^{11}C isotope. Our studies focused on developing a route to an agent that would incorporate ^{18}F, which has a longer half-life (110 min). We chose to examine the core of SCH 442416 as a starting point since it had already been demonstrated to cleanly cross the blood/brain barrier as well as possessing high A$_{2A}$ AR
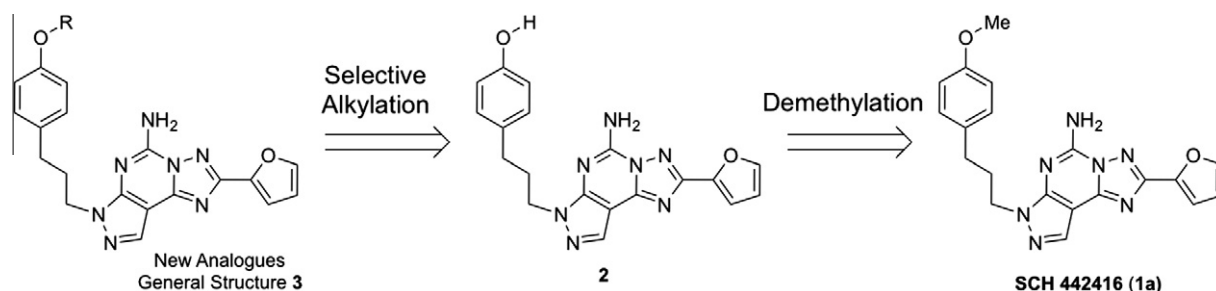
Chart 1. Antagonist ligands of the pyrazolo[4,3-e]-1,2,4-triazolo[1,5-c]pyrimidine class that have been in development for the treatment of PD.

Scheme 1. Retrosynthetic strategy for facile preparation of analogues.

selectivity over the A_1 and A_3 ARs. In this study, we shall describe our modeling, preparation, and SAR studies of a new set of A_{2A} AR ligands.

A_{2A} ARs are G protein-coupled receptors (GPCR) with a defined binding site for an antagonist. The X-ray structure of the A_{2A} AR in complex with the triazolotriazine ZM241385, a high affinity A_{2A} selective antagonist,[10] was recently released (PDB ID: 3EML) and used here as a basis for ligand docking.[11] The coordinates of the A_{2A} AR crystal structure were used to investigate the binding properties of fluoroethyl ligand **5** (Table 1). The active pocket of A_{2A} AR is located in the transmembrane (TM) bundle, involving residues from TM3, TM5, TM6, and TM7. Residues from the second and third extracellular loops (EL2 and EL3) also delineate the upper part of the binding cavity (Fig. 1a). A flexible docking of ligands in the binding site for adenosine of the A_{2A} AR was performed using the Induce Fit Docking (IFD) protocol in the Schrödinger software package.[12] This protocol combines the flexible docking, by means of the GLIDE docking program,[13] of the ligands in the active site and the refinement, by means of the Prime module,[14] of the binding site residues in order to accommodate the correct binding conformation of the ligands. Our IFD model of the fluorinated analog **5** shows a binding mode similar to the co-crystallized ZM241385 conformation reproducing the key interactions that were observed in the X-ray structure of the A_{2A} AR with residues like N253 in TM6 and E169 and F168 in EL2 (see Experimental section for amino acids numeration). The orientation adopted by the pyrazolotriazolopyrimidine analogues is almost perpendicular to the cell membrane plane (Fig. 1a). The exocyclic amino group of the heterocyclic unit makes strong H-bond interactions with the side chains of N253 and E169. The central pyrazolotriazolopyrimidine core forms an aromatic π-stacking with the phenyl side chain of F168 in EL2 and other hydrophobic interactions with the side chains of L249 in TM6 and I274 in TM7 (Fig. 1b). The furan ring is engaged in polar and hydrophobic interactions with N253, H250 and W246 in TM6, and M177 in TM5. The substituted phenolic side chain of the pyrazolotriazolopyrimidine derivatives is located in the extracellular region of the binding pocket. The phenyl–propyl linker is embedded by hydrophobic residues such as L167 in EL2, H264 in EL3, L267 and M270 in the extracellular part of TM7. The terminal phenolic side chains (–OR, Scheme 1)

protrude towards a more polar, solvent exposed area at the top of the receptor. A conformational flexibility was detected for the terminal phenolic side chains, and substituents larger than the methoxy group, in our fluorinated compounds series, were found to be well tolerated in the docking models (Fig. 1 shows fluoroethyl analogue **5**). The modeling results, combined with the know ability of SCH 442416 to cross the blood brain barrier,[7] encouraged us to explore the structural variability that is tolerated on the phenolic position.
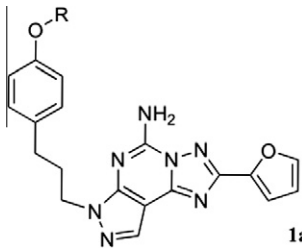
It was envisioned that elaboration of the phenoxymethyl moiety into larger ether substituents would be well tolerated by the A_{2A} AR. To prepare our new analogues of SCH 442416, we tested the approach that a family of compounds could arise from a common phenolic intermediate (**2**) via selective alkylation of the phenol in the presence of the nucleophilic aromatic amine core under basic conditions. The initial phenol (**2**) would be prepared from commercially available SCH 442416 through a nucleophilic demethylation. This concise route would allow the facile preparation and screening of new analogues.

We were gratified to find that demethylation of SCH 442416 (**1**) proceeded in near quantitative yield with boron tribromide to provide known phenol **2** (Scheme 2).[15,16] With phenol **2** in hand, we examined a variety of conditions for the selective alkylation of the phenol. Alkylation of the phenol was achieved in high regio- and chemoselectivity using methanol as the solvent. Alternate solvents were substantially less efficacious. Polar aprotic solvents, such as DMF, lead to contamination with polyalkylation and/or decomposition, while solubility was poor in other alcoholic/ketonic solvents. A variety of bases furnished the desired products (such as Bu_4NOH, K_2CO_3, and others) but Cs_2CO_3 provided the highest yields and cleanest reaction mixtures. It was found that highly selective alkylation of the phenol could be obtained with Cs_2CO_3 as the base in a solution of methanol for a variety of electrophiles including primary, secondary and allylic bromides. Using the optimized reaction conditions, we were able to produce a family of new analogues (Scheme 2).

During our alkylation studies, we wished to access the homologated glycolated product **13** and corresponding mesylate **14** (Scheme 3). It is reasonably well precedented that this can be obtained directly through reaction with ethylene oxide,[17] ethylene

Table 1
Affinity of a series of pyrazolotriazolopyrimidine derivatives at three subtypes of ARs in various species

Compound	R	Affinity (K_i, nM, or % inhibition at 10 µM)		
		$A_1{}^a$ (%)	$A_{2A}{}^a$ (nM)	$A_3{}^a$ (%)
1a	–Me	38.4 ± 1.9	4.1 ± 0.4	67.4 ± 0.5
2	–H	44.3 ± 0.9	48.3 ± 28	34.2 ± 2.6
4	–Et	4.8 ± 3.3	43.9 ± 9.3	4940 ± 1700[b]
5	–CH$_2$CH$_2$F	42.7 ± 0.6	12.4 ± 0.8	59.6 ± 4.7
6	–n-Pr	17.9 ± 3.1	11.7 ± 2.2	36.5 ± 5.6
7	–i-Pr	35 ± 4.6	13.3 ± 2.6	72.8 ± 3.8
8	–sec-Bu	16.8 ± 2.8	22.1 ± 0.4	41.9 ± 3.0
9	–Allyl	32.8 ± 1.2	9.0 ± 2.3	62.5 ± 2.3
10	–Homoallyl	25.5 ± 1.3	14.4 ± 5.2	44.8 ± 0.8
11	–Cinnamyl	7.3 ± 2.7	308 ± 141	17.8 ± 3.4
12	–Hydrocinnamyl	6.9 ± 2.0	78.9 ± 15.5	18.2 ± 2.6
13	–CH$_2$CH$_2$OH	47.9 ± 8.2	23.9 ± 3.3	57.8 ± 6.4
14	–CH$_2$CH$_2$–OMs	27.8 ± 6.2	45.7 ± 9.4	62.4 ± 1.7

^{a} All experiments were done on CHO or HEK293 (A_{2A} only) cells stably expressing one of three subtypes of human ARs. The binding affinity for A_1, A_{2A} and A_3ARs was expressed as K_i values ($n = 3$–5) and was determined by using agonist radioligands ([^{3}H]CCPA; [^{3}H]CGS21680; or [^{125}I]I-AB-MECA, respectively), unless noted.
^{b} K_i expressed as nM.
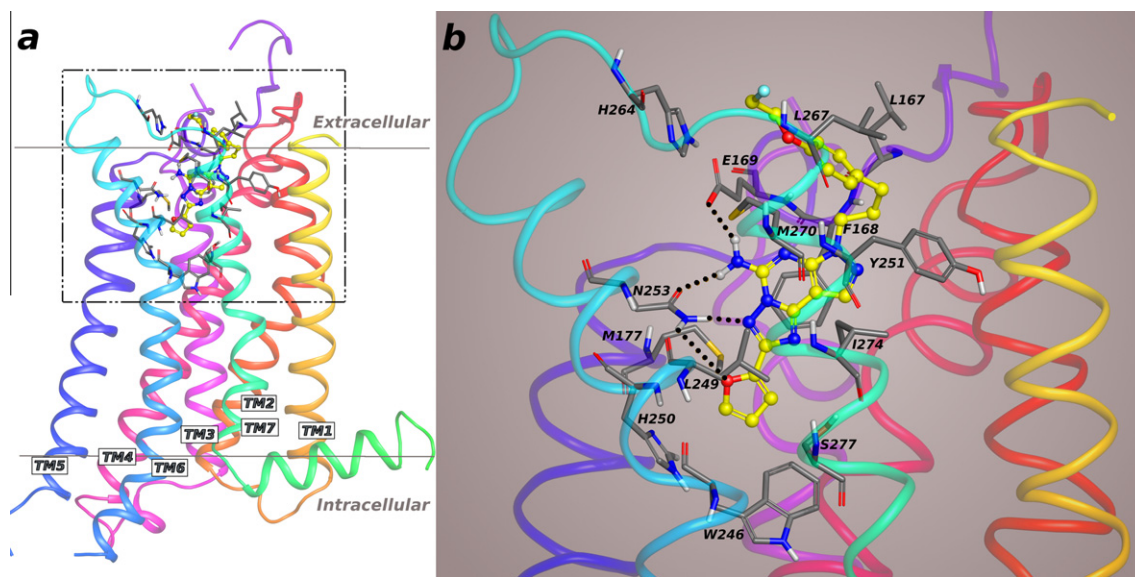
Figure 1. Docking pose of fluorinated analogue **5** in the binding pocket of the A_{2A} AR. Panel a: view from the plane of the cellular membrane of the crystallographic structure of A_{2A} AR bound to the ligand. The binding pocket is located in the TM bundle region of the receptor defined by residues from TM3, TM5, TM6, and TM7 and residues from EL2 and EL3. Panel b: Close-up view showing the best scoring pose for compound **5** in the active pocket of A_{2A} AR. The ligand is anchored to the residues in the binding pocket by strong H-bond interactions and stabilized by hydrophobic interactions. In the image the carbon atoms are colored gray for the protein and yellow for the ligand. The non-polar hydrogen atoms are not shown for clarity. Key interactions of side chains residues within the binding site are highlighted as dotted lines.

oxide precursors such bromoethanol,[18] or through a sequence of reactions with ethyl iodoacetate follow by reduction/deprotection.[19] We found that the homologation reaction was more complicated in the presence of the reactive heterocyclic core. However, fluoroethanol with tetrabutylammonium hydroxide provided a good isolated yield of glycol **13** with the fewest side products. This was an unexpected discovery, because fluoroethanol has not been previously reported as a precursor to ethylene oxide. Although glycol **13** can be isolated via preparative TLC, it was found that direct submission of the highly polar unpurified glycol **13** to mesylation conditions furnished **14** in 42% isolated overall yield for the two steps.

Binding assays at three hAR subtypes were carried out on the 1,2,4-triazolo[1,5-c]pyrimidine derivatives using standard radioligands and membrane preparations from Chinese hamster ovary (CHO) cells (A_1 and A_3) or human embryonic kidney (HEK293) cells (A_{2A}) stably expressing a hAR subtype (Table 1).[20–23]
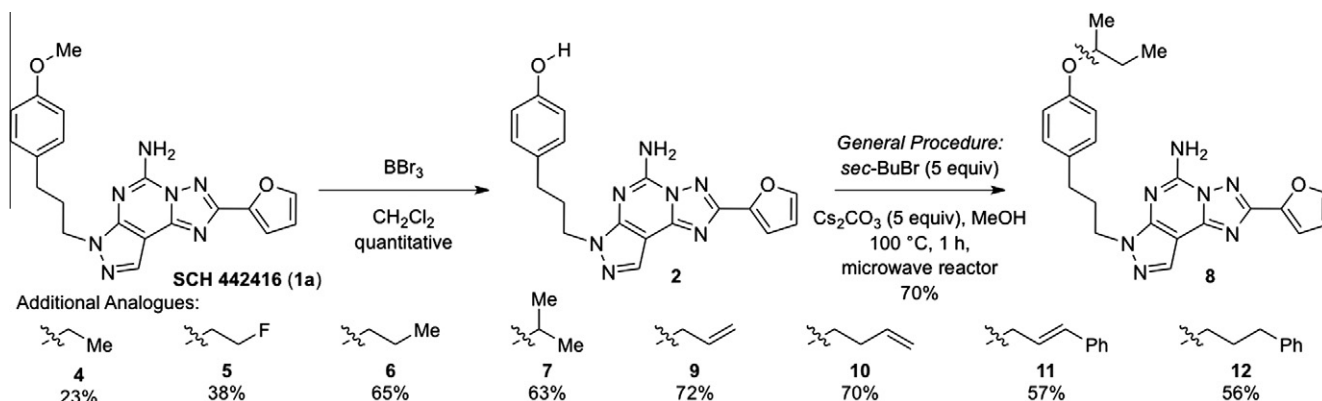
Scheme 2. Rapid and facile synthetic preparation of SCH 442416 analogues.
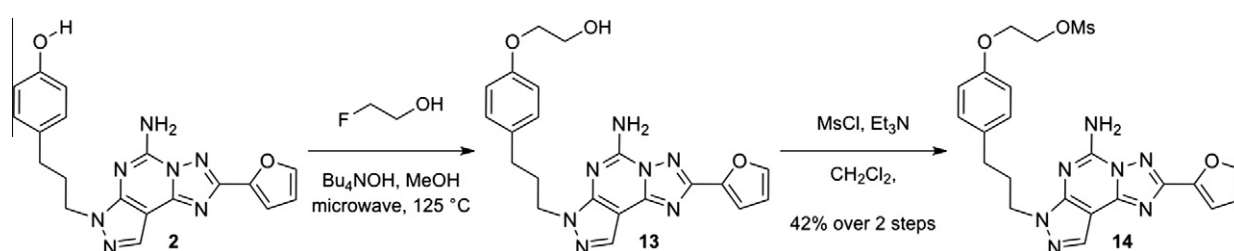
Scheme 3. Glycolation of phenol **2** with fluoroethanol.

In general, our substrates show that there is a wide range of structural tolerance of substitution on the phenolic position. The newly synthesized analogues gave binding inhibition constants (K_i) in the range of 9.0–300 nM (Table 1), which is consistent with the observed binding affinity of SCH 442416 (**1a**), which was measured to be 4.1 nM.[24] These results agree with the ligand docking, which indicated that the phenolic substituent protrudes toward the extracellular matrix and is close to the flexible extracelluar loops of the A_{2A} AR.

Small structural variation of the phenoxy substituent gave analogues with binding affinity similar to the parent ligand. It was found that removal of the –methyl substituent from the phenoxy position resulted in reduced binding affinity, while simple *n*-alkyl (saturated and unsaturated analogues) retained activity as the chain length increased. Addition of a fluorine to an ethyl substituent (ligand **5**) displayed comparable binding relative to the unsubstituted ethyl (**4**) and the *n*-propyl (**6**) analogues. The *O*-fluoroethyl analogue **5** appeared to be suitable for use as a PET tracer based on its favorable binding affinity. It displayed a K_i value of 12.4 nM at the A_{2A} AR and was highly selective in comparison to the A_1 and A_3 ARs, at which the affinities were estimated to be approximately 10 μM. The preparation of [18]F-**5** and studies of its use as a PET tracer have been completed and will be reported elsewhere.[25]

As the size of the substituent increased (–R, Table 1), variation was observed in the binding affinity. Alpha branching did not dramatically affect the affinity (*i*-Pr analogue **7** and *s*-Bu analogue **8**) nor did the introduction of polarity to a short chain (hydroxylethyl analogue **13** and mesylate analogue **14**). Although, cinnamyl derivative **11** and hydrocinnamyl derivate **12** are tolerated, they show a reduced binding affinity at the A_{2A} AR. The observed reduction in affinity may be a function of the non-polar character of these groups, which necessarily project into the polar extracellular loop region (Fig. 1). Due to the polar character of this loop region, it may be expected to better accept charged and/or H-bonding substituents as compared to aromatic rings. Future experiments will examine more polar side chains to evaluate what functionality is most complementary to the polarity of this region.

We have synthesized a family of A_{2A} AR ligands, based on the known antagonist, SCH 442416 (**1a**), which has structural variability on the side chain phenolic terminus (including –Et, –*i*-Pr, –allyl, and others). Our facile preparation of this family of A_{2A} antagonists was achieved through a highly phenol-selective alkylation in the presence of nucleophilic heterocyclic core. The binding properties of the newly prepared analogues were consistent with our predictions based on molecular modeling of these antagonists with the A_{2A} AR. The goal of preparing a fluorine-substituted A_{2A} selective ligand was achieved with the fluoroethyl analogue **5**. The preparation of the ^{18}F-labeled ligand and its utility as a PET ligand are the subject of ongoing studies.[25]

Acknowledgements

Supplementary data

Supplementary data associated with this article can be found, in the online version, at doi:10.1016/j.bmcl.2010.08.021.

References and notes

1. Pinna, A. *Expert Opin. Invest. Drugs* **2009**, *18*, 1619.
2. The Huntington's Disease Collaborative Research Group *Cell* **1993**, *72*, 971.
3. Schwarzschild, M. A.; Agnati, L.; Fuxe, K.; Chen, J. F.; Morelli, M. *Trends Neurosci.* **2006**, *29*, 647.
4. Todde, S.; Moresco, R. M.; Simonelli, P.; Baraldi, P. G.; Cacciari, B.; Spalluto, G.; Varani, K.; Monopoli, A.; Matarrese, M.; Carpinelli, A.; Magni, F.; Kienle, M. G.; Fazio, F. *J. Med. Chem.* **2000**, *43*, 4359.
5. Neustadt, B. R.; Hao, J.; Lindo, N.; Greenlee, W. J.; Stamford, A. W.; Tulshian, D.; Ongini, E.; Hunter, J.; Monopoli, A.; Bertorelli, R.; Foster, C.; Arik, L.; Lachowicz, J.; Ng, K.; Feng, K.-I. *Bioorg. Med. Chem. Lett.* **2007**, *17*, 1376.
6. Hodgson, R. A.; Bertorelli, R.; Varty, G. B.; Lachowicz, J. E.; Forlani, A.; Fredduzzi, S.; Cohen-Williams, M. E.; Higgins, G. A.; Impagnatiello, F.; Nicolussi, E.; Parra,

L. E.; Foster, C.; Zhai, Y.; Neustadt, B. R.; Stamford, A. W.; Parker, E. M.; Reggiani, A.; Hunter, J. C. *J. Pharmacol. Exp. Ther.* **2009**, *330*, 294.

7. Moresco, R. M.; Todde, S.; Belloli, S.; Simonelli, P.; Panzacchi, A.; Rigamonti, M.; Galli-Kienle, M.; Fazio, F. *Eur. J. Nucl. Med. Mol. Imaging* **2005**, *32*, 405.
8. Ramlackhansingh, A. F.; Bose, S. K.; Ahmed, I.; Turkheimer, F. E.; Pavese, N.; Brooks, D. J. *Neurology* **2010**, *74*, A588.
9. SCH 420814 (with the trade name Preladenant) recently completed a phase II trial. ClinicalTrials.gov Identifier: NCT00537017.
10. Palmer, T. M.; Poucher, S. M.; Jacobson, K. A.; Stiles, G. L. *Mol. Pharmacol.* **1995**, *48*, 970. PMID 8848012.
11. Jaakola, V.-P.; Griffith, M. T.; Hanson, M. A.; Cherezov, V.; Chien, E. Y. T.; Lane, J. R.; IJzerman, A. P.; Stevens, R. C. *Science* **2008**, *322*, 1211.
12. Sherman, W.; Day, T.; Jacobson, M. P.; Friesner, R. A.; Farid, R. *J. Med. Chem.* **2006**, *49*, 534.
13. GLIDE, *version 5.0, Schrödinger*, LLC, New York, NY, 2005.
14. *Prime, version 2.0, Schrödinger*, LLC, New York, NY, 2005.
15. McOmie, J. F. M.; Watts, M. L.; West, D. E. *Tetrahedron* **1968**, *24*, 2289.
16. Baraldi, P. G.; Cacciari, B.; Spalluto, G.; Bergonzoni, M.; Dionisotti, S.; Ongini, E.; Varani, K.; Borea, P. A. *J. Med. Chem.* **1998**, *41*, 2126.
17. Eichinger, P. C. H.; Bowie, J. H.; Hayes, R. N. *J. Am. Chem. Soc.* **1989**, *111*, 4224.
18. Tsotinis, A.; Calogeropoulou, T.; Koufaki, M.; Souli, C.; Balzarini, J.; De Clerq, E.; Makriyannis, A. *J. Med. Chem.* **1996**, *39*, 3418.
19. Nittoli, T.; Curran, K.; Insaf, S.; DiGrandi, M.; Orlowski, M.; Chopra, R.; Agarwal, A.; Howe, A. Y. M.; Prashad, A.; Floyd, M. B.; Johnson, B.; Sutherland, A.; Wheless, K.; Feld, B.; O'Connell, J.; Mansour, T. S.; Bloom, J. *J. Med. Chem.* **2007**, *50*, 2108.
20. Klotz, K. N.; Lohse, M. J.; Schwabe, U.; Cristalli, G.; Vittori, S.; Grifantini, M. *Naunyn-Schmiedebergs Arch. Pharmacol.* **1989**, *340*, 679.
21. Jarvis, M. F.; Schutz, R.; Hutchison, A. J.; Do, E.; Sills, M. A.; Williams, M. *J. Pharmacol. Exp. Ther.* **1989**, *251*, 888.
22. Olah, M. E.; Gallo-Rodriguez, C.; Jacobson, K. A.; Stiles, G. L. *Mol. Pharmacol.* **1994**, *45*, 978.
23. Bradford, M. M. *Anal. Biochem.* **1976**, *72*, 248.
24. Kecskés, M.; Kumar, T. S.; Yoo, L.; Gao, Z. G.; Jacobson, K. A. *Biochem. Pharmacol.* **2010**, *80*, 506.
25. Bhattacharjee, A.; Lang, L.; Jacobson, O.; Shinkre, B. A.; Ma, Y.; Shi, Y.; Gao, Z.; Trenkle, W. C.; Jacobson, K. A.; Kiesewetter, D. O. 'Imaging of F-18 labeled adenosine A$_{2A}$ receptor antagonist in the rat striatum with positron emission tomography' presented at the Society for Neuroscience National Meeting, Neuroscience 2009, Chicago, IL, Oct 18, 2009, Program 239.5.